A microcapillary rheometer for microliter sized polymer characterization

Daniele Tammaro [a,b,*], Gaetano D'Avino [b], Salvatore Costanzo [b], Ernesto Di Maio [b], Nino Grizzuti [b], Pier Luca Maffettone [b]

[a] DPI, P.O. Box 902, 5600, AX Eindhoven, the Netherlands
[b] Dipartimento di Ingegneria Chimica, dei Materiali e della Produzione Industriale, University of Naples Federico II, P. le Tecchio 80, I-80125, Napoli, Italy

ARTICLE INFO

ABSTRACT

We report the design of a microcapillary rheometer (μCR) that allows to perform experiments rapidly and in a broad range of shear rates (i.e., from 0.1 to 1000 s^{-1}), using small amounts of material (i.e., just few milligrams). Additionally, multiple measurement parallelization makes it suitable for High-Throughput Rheological Experimentation (HT-Rheo-E) of polymer melts. The novel rheometer consists of a set of three cylindrical microcapillaries in which the fluid flows driven by a controlled pressure. A camera, placed at the capillary exit, records the fluid motion to measure its flow rate, from which the fluid viscosity can be determined. The optimization of the setup allowed for reliable and fast viscosity measurements using ca. 10 mg of material. The current work reports the design of the rheometer and validation measurements on several model fluids. The microfabricated μCR is of potential interest for applications in quality control and research where rapid and repeated measurements using limited milligrams of polymer are required, as well as for High-Throughput-Experimentation of complex fluids (e.g., biological systems).

1. Introduction

Material design, development and production are predominantly carried out via single trial-and-error experiments guided by human intuition and previous knowledge. This approach is time consuming and produces a wide amount of waste. The concept of gradient libraries and systematic parallel screening for desired material properties to accelerate their discovery was introduced by the pioneering work of Hanak in the 1970s and a comprehensive historical review on the early years of High Throughput Experimentation (HTE) has been recently presented by Kumar et al. [1,2]. The parallel screening by means of HTE can be enhanced through data science-based methods (e.g., artificial intelligence) and allows to shed light on the relationships between material synthesis variables (such as composition) and measurable material properties (such as processability, viscosity, etc.). The HTE approach has been recently applied to the rheology (HT-Rheo-E) of emulsions and low viscous fluids by means of microrheometry using miniaturized channels [3].

The term microrheometry has been employed by numerous authors to refer to a large number of different experimental configurations [4,5]. In general, microrheometry may be defined as the area of rheometry for measuring quantitatively the rheological properties of a fluid polymer when at least one characteristic dimension is on the scale of micrometers, so that small quantities of fluid can be used [6]. A first attempt to perform experiments in parallel was reported by Moon et al. [7], who developed a multi-sample micro-slit rheometer for simultaneous measurements on different polymers, and two direct methods to simultaneously measure the dynamic capillary pressure and the viscosity of fluids by application of differential forces during flow into microchannels. Their calculation of the viscosity from the polymer front flow, however, was not fast, with a time-consuming, long cleaning procedure needed after each experiment [8]. Data reduction from the polymer melt behaviour inside the microcavity during flow was cleverly tackled, though remaining not an easy task.

At the microscale, some factors that are normally neglected at the macroscale may play an important role [9]. Wall effects are typically more relevant in systems with large surface-to-volume ratios. The use of standard capillary rheometry with submillimeter geometries has been discussed by Benbow and Lamb [10], who considered the range of obtainable stress and viscosity, and by Ybarra [11] in terms of the advantageous effects of reduced shear heating and the need to consider pressure induced changes in viscosity. Shidara [12] described extrudate

instabilities and slip that may become more important at microscale. Clasen and McKinley [13] performed a thorough and systematic study on the effect of the characteristic size of microchannels (from 100 down to 3 μm) on the viscometric properties. They found that, for Newtonian and non-Newtonian particle suspensions and emulsions, there is an effect of the channel size only when it becomes comparable with the particle/droplet size. Above that size, the behaviour of polymer solutions and melts is not affected by the channel dimensions. Despite the progresses, the above-mentioned limitations motivate the development of a micro-rheometer truly allowing for HT-Rheo-E.

A novel rheometer should satisfy two main purposes: a) to supply information on process-oriented rheology of complex fluids, thus allowing for the measurement of the so-called nonlinear response, i.e., high shear rates; b) to perform experiments in the line of HT-Rheo-E. Here, we propose a simple and cost-effective rheometer for fast and reliable characterization of complex liquids that uses a small amount of fluid and is capable of performing experiments in parallel to maximize data production rate. The innovative apparatus is based on the optical measurement of the flow rate of a few-milligram polymer flowing under the action of a pressurized gas. Fast operations are accessible by using microcapillaries inserted in a metal chamber. The reduction of experimental time is a relevant feature aiming at HT-Rheo-E. Fast measurement also minimizes thermal degradation, an important aspect when characterizing degradable polymers. The proposed microcapillary rheometer (μCR) allows for an optimal control of the polymer temperature and flow conditions on several decades of shear rates using from 2 up to no more than 50 mg of polymer in a fast and simple way. Furthermore, the flexibility of the device design also allows for the characterization of other properties, such as surface tension, contact angle, and (possible) melt fracture.

2. Design considerations

The rheometer is a pressure driven, stress-imposed device that has been designed to achieve the following objectives: i) to properly work at high temperatures and pressures to characterize highly viscous polymer melts; ii) to use using milligram size polymers; iii) simplicity, cost-effective, and parallel measurements. Table 1 reports the relevant dimensionless numbers to be accounted for the design of the μCR. The quantification of the typical ranges of those dimensionless groups is based on characteristic data for a polymer melt (for example, PS at 200 °C: viscosity, η, 10^3 Pa s, velocity, V, 10^{-2} m/s, surface tension, σ, 10^{-2} N/m, density, ρ, 10^3 kg/m^3, capillary diameter, D, 10^{-4} m, thermal conductivity, k, 10^{-2} W/mK). From which we have:

a) $Re \ll 1$, i.e., negligibility of inertial effects, implies small capillary diameters to reduce the characteristic transient time, $\tau_i = \frac{\rho D^2}{\eta} (\approx 10^{-8} s$, for the reference polymer cited above). This allows to optimize the experimental time, and through the application of a stepwise pressure ramps it is possible to span a wide range of shear rates with the same polymer and to measure the corresponding steady-state viscosities.

b) $Ga \ll 1$ and $Ca \gg 1$ so as to neglect capillary and gravitational forces with respect to viscous forces. As a consequence, the total pressure drop, ΔP, along the capillary can be written as [14]: $\Delta P = P_{vis} + P_\sigma + P_g \cong P_{vis}$; where P_{vis}, P_σ, P_g are the contributions of viscous, capillary, and gravity forces, respectively.

c) $Na < 1$ (from 0.04 to 0.9 for our reference polymer), to make the dissipative heating effect negligible [15].

It is well known that in capillary rheometer the entrance and exit loss should be considered for an accurate measurement of viscosity. An experimental procedure for the correction proposed by Bagley [16]. Even if it is a simple procedure, it requires material for numerous tests at different capillary land lengths, which is in contrast with the objective of measuring rheological properties with a small amount of polymer. It is also well known that the end loss becomes negligible for capillaries with large land length. In order to reduce the amount of material and measurement time, a sufficiently large land length can be designed so that the end pressure can be considered negligible [17]. In the case of viscoelastic fluids, the entrance and exit loss can be seen as composed of viscous and elastic components [18]. However, Metzner and White (1965) concluded that the elastic effects due to profile development are a small part of the elastic component of the pressure drop and hence can be taken as negligible [19].

3. MicroCapillary rheometer (μCR)

In designing our microcapillary, we decided to avoid devices where a piston is driven either hydraulically, mechanically or by means of a weight, because errors due to friction or leakage of material past the piston are enhanced by the large surface-to-volume ratio in a small diameter reservoir. The proposed μCR consists of cylindrical microcapillaries in which the fluid is made to flow by a controlled gas pressure. It is made of three custom-designed pieces fabricated by Roman Weber GmbH (Tobel, Switzerland), schematized in Fig. 1a. The microcapillaries (diameter D and land length L) are in the central part, which is made of brass for its high thermal conductivity. The number of microcapillaries can be increased at will, depending on the number of desired tests to be performed in parallel (e.g., different temperatures, different polymer grades, etc.). Herein, we present the results obtained with two different designs: one having three holes with the same diameter D = 400 μm and different land length, L, with L/D = 5, 7.5, 10 (Fig. 1e); the other with just a single hole with diameter D = 70 μm and a L/D = 13. A reservoir with diameter D_r = 2 mm and a converging section to facilitate sample loading is placed above the microcapillary (Fig. 1a). This central part is assembled with the top part (Fig. 1a) characterized by 3 ports for: gas inlet, a pressure sensor (PR-23SYEi/-1, from Keller, Germany) and a temperature sensor (RTD Pt100 from RS, UK). The top part sinks into the fluid reservoir. The temperature of brass piece is controlled by a band heater operating in conjunction with a thermocouple (T1) read by a thermo-regulator (Ascon-New England Temperature Solutions, Attleboro, MA, model X1). Temperature is checked uniformity along the microcapillary is measured by placing two thermocouples in the metal near the sample holders (T2) and inside the polymer with a Pt100 entering from the top (T3). Temperature data are recorded via software (i.e. LabviewTM software, National Instrument, Texas, United States) on a computer. For typical experimental conditions, from ambient temperature up to 200 °C, we measured differences between T2 and T3 within 1.5 °C. The time needed for heating the polymer from room conditions to a typical temperature (say 200 °C) is approximately 15 min.

The exit chamber (bottom part) is screwed to the central part and is equipped with two transparent high pressure windows (1/2" NPT 3IlFU from Precision Sapphire Technologies, Lithuania), with an opening

Table 1
Dimensionless numbers helping in the designing phase.

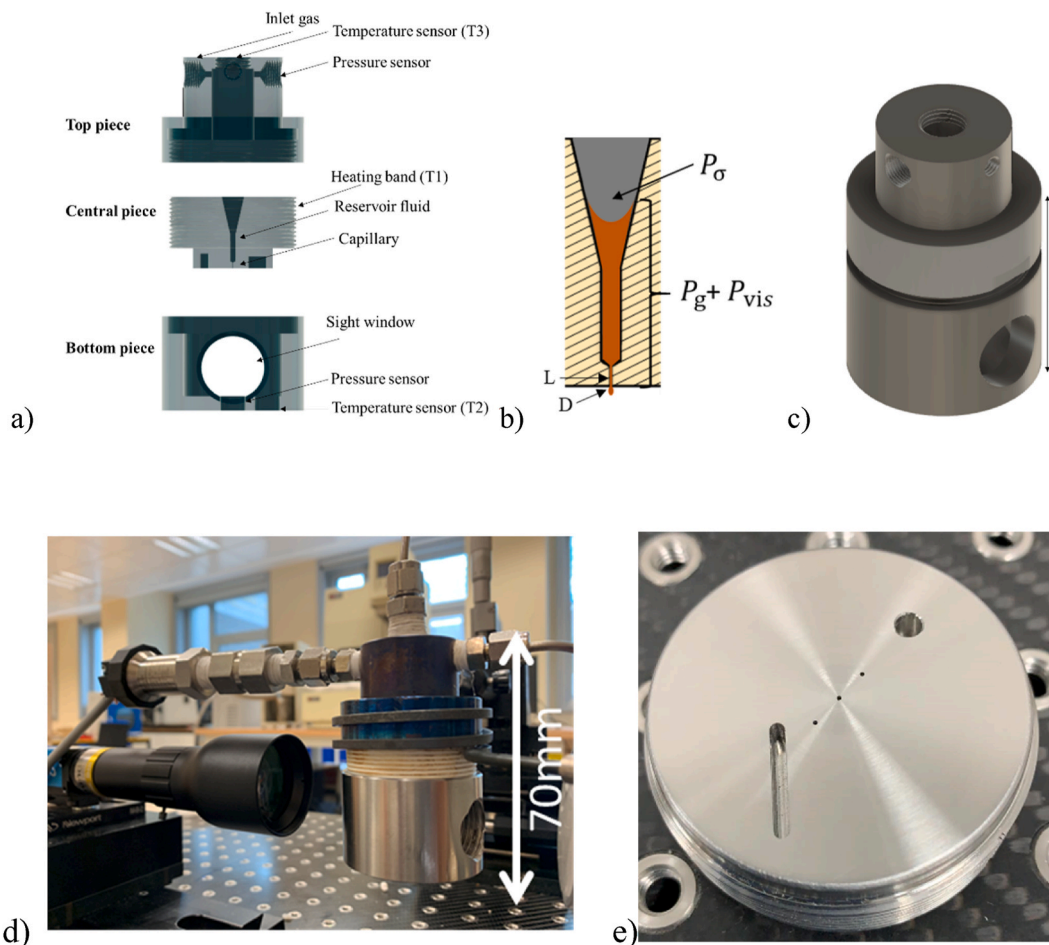| Dimensionless number	Notation	Formula	Meaning	Value
Capillary number	Ca	$Ca = \dfrac{V\eta}{\sigma}$	$\dfrac{viscous\ force}{capillary\ force}$	$Ca \gg 1$
Reynolds number	Re	$Re = \dfrac{\rho V D}{\eta}$	$\dfrac{inertia\ force}{viscous\ force}$	$Re \ll 1$
Galileo number	Ga	$Ga = \dfrac{\rho g D^3}{\eta^2}$	$\dfrac{gravity\ force}{viscous\ force}$	$Ga \ll 1$
Nahme number	Na	$Na = \dfrac{\eta \beta V^2}{k}$	$\dfrac{heat\ by\ viscous\ dissipation}{heat\ by\ conduction}$	$Na < 1$

Fig. 1. a) 3D rendering of top, central and bottom piece, b) sketch of the fluid filling the microcapillary and the reservoir (*D* and *L* are diameter and land length of the microcapillary, c) 3D rendering of the full assembly, d) picture of the assembled setup and e) manufactured multi-microcapillaries plate.

diameter of 12 mm, and two ports for temperature and pressure measurements. The entire assembly is shown in Fig. 1c and d. Its dimension and weight make the setup a transportable lab on desk apparatus.

As mentioned in the Introduction, the flow rate is measured via optical imaging. To this end, a videocamera (DMX TIS 1/1,8″ CMOS 3072x2048 Monocro from DB Electronics, Italy) equipped with an optical lens (2,0X, 2/3" SilverTL Telecentric Lens from Edmund, UK) is aligned at the capillary exit to record the fluid flow. The use of the 2.0x optical lens allows a resolution of 0.3microns for the calculation of the volumetric flow rate. The background is illuminated by a diffused light. Once the volumetric flow rate, *Q*, is measured and the pressure history recorded, the apparent viscosity calculation is possible.

For pressure control, nitrogen gas flows from the regulator of a standard nitrogen cylinder at 200 bar into the top chamber of μCR through a solenoid valve (SCG238A046-24VCA, 2 port, NC, 24 V ac, 1/2in, EMERSON–ASCO, UK) that is software actuated. The reading of the pressure transducer is recorded with a frequency of 50 data points per second, and the pressure sensitivity is 0.05% of the nominal calibrated full-scale.

The experimental procedure consists of: I) sample loading (shown in Supplementary Video 1), II) temperature rise and stabilization, III) application of nitrogen pressure and, in parallel, optical determination of the volumetric flow rate through camera recording. In case of fluids prone to degradation, the top and bottom chambers are flushed with nitrogen during the heating phase. It is worth to say that the typical time of an experiment (ca. 2 min) is much smaller than the diffusion time of nitrogen in millimetres characteristic scale [10]. The possibility to control the pressure and the temperature in the exit chamber allows to

perform rheological experiment at high pressure to investigate the dependence of viscosity and contact angle on the pressure.

Supplementary video related to this article can be found at htt ps://doi.org/10.1016/j.polymertesting.2021.107332

4. Materials to test the μCR

Three model fluids were selected to test the rheometer: a polydimethylsiloxane (PDMS, PSF-1000000cSt Silicone Fluid from ClearCo), a polystyrene (PS, grade N8100 supplied by Versalis, Italy), and an ethylene/1-octene statistical multi-block copolymers (POE) produced by the Dow Chemical Company (commercial grade name POE d9007, [20]. Nitrogen in high pressure bottles with a purity of 99% (supplied by Aircos, Italy), was used to impose the pressure.

5. Optical measurement

The μCR was tested with PDMS at 25 °C and PS at 180 °C to measure their viscosities in a wide range of shear rates. When the solenoid valve is opened the nitrogen pressurizes the top chamber (phase I in Fig. 2b) and the pressure eventually reaches a constant value (phase II in Fig. 2b). Two testing procedures can be performed: a) constant pressure test (Fig. 2a and b) and b) pressure sweep test (Fig. 2c). The camera records the fluid flow at the exit from the three microcapillaries (Fig. 2a) and the volume as a function of time is calculated for the three strands by image analysis, by assuming axial symmetry of the 2D profile (Fig. 2b) [24]. The error due to the axial symmetry assumption is detailed below, in the section about the error analysis. The volume is obtained by
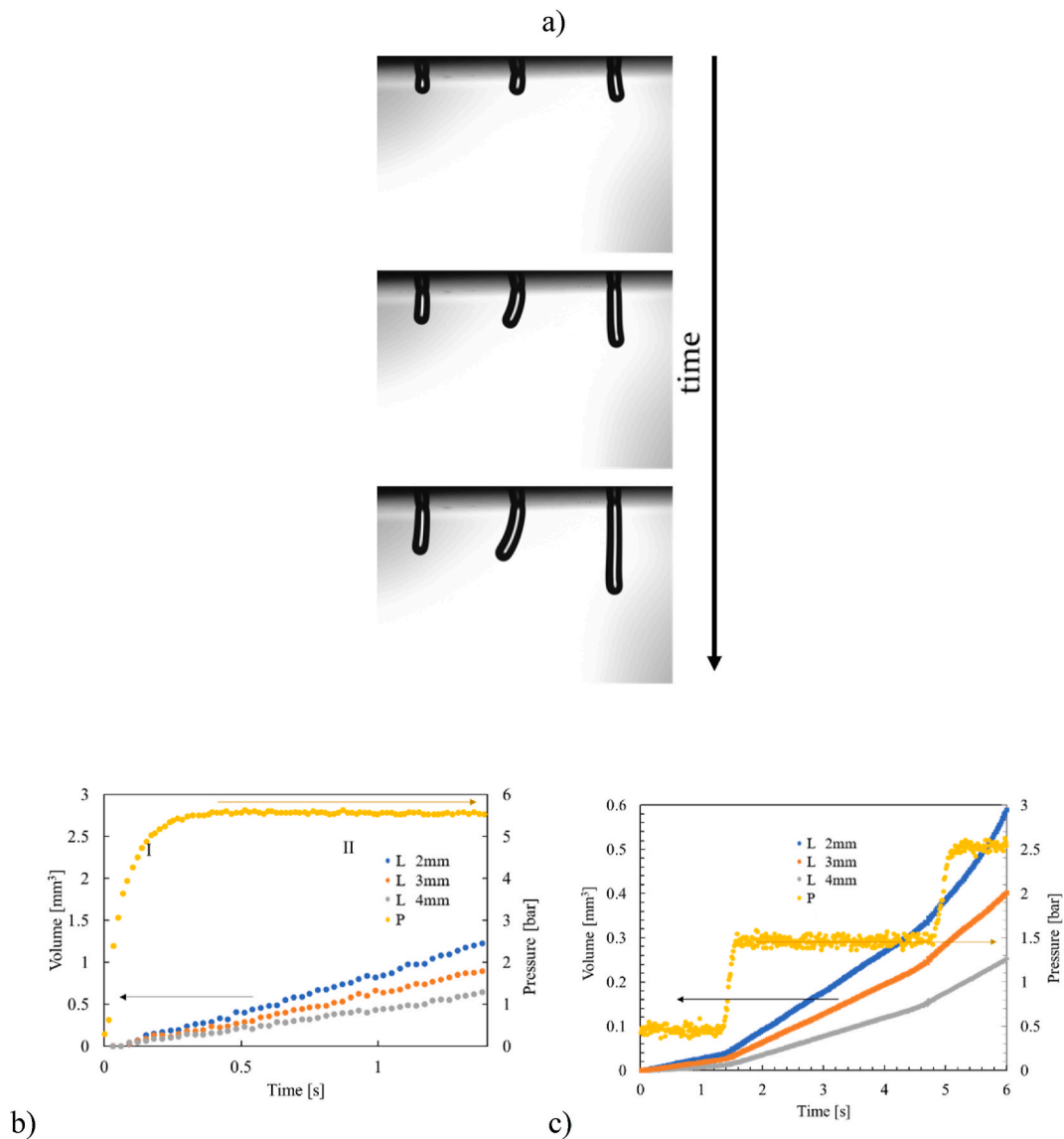
Fig. 2. a) snapshots of the polymer strand at the microcapillary exit; b) constant pressure experiment (yellow circles are the pressure, blue, red and grey circles are the strand volumes for L = 2, 3, 4 mm respectively); c) pressure sweep experiment (yellow circles are the pressure, blue, red and grey circles are the strand volumes for L = 2, 3, 4 mm respectively). (For interpretation of the references to colour in this figure legend, the reader is referred to the Web version of this article.)

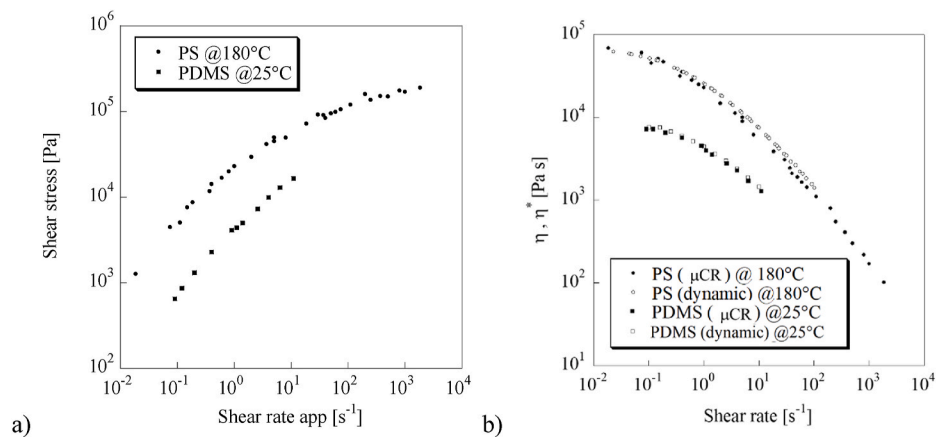
Fig. 3. a) The shear stress as a function of the apparent shear rate obtained from the μCR; b) the viscosity as a function of the true shear rate after the Rabinowitsch correction. Open symbols are from small amplitude oscillatory dynamic measurements and closed symbols are from the μCR.

integration of the strand profile via Labview software. The video of a typical test with three capillaries is reported in the Supplementary Video 2. An example of sweep pressure test is shown in Fig. 2c, where the constant slope of the volume (i.e.V(t)) signal is indicative of a constant, steady-state flow rate.

The bend of the middle extrudate, visible in Fig. 2a, is under investigation and it will be studied in greater details in a future work.

6. Results and discussion

The flexibility of the µCR opens up to a series of measurements that can be performed with the same instrument by using only just a few milligrams of polymers. In the following section we present the measurements of: a) viscosity, b) die swell, c) surface properties (e.g., contact angle) and d) melt fracture.

7. Viscosity

The shear stress at the capillary wall ($\tau_w = \frac{R\,P}{2\,L}$) as a function of the apparent shear rate ($\dot{\gamma}_a = \frac{4\,Q\,P}{\pi\,R^3}$) is plotted in Fig. 3a for PS and PDMS samples. Using the Weissenberg-Rabinowitsch correction [21], the true shear rate is calculated, and the corresponding viscosity is plotted in Fig. 3b. The calculation of the viscosity is directly linked to the measured flow rate and pressure without additional measurements needed.

The results for PS at 180 °C and PDMS at 25 °C are compared with dynamic measurements obtained in a conventional rotational rheometer (Anton Paar MCR702, Germany) assuming the validity of the Cox-Merz rule [17]. Good agreement between the two measurements is observed with an error of 7% for a confidence interval of 95%. Our findings confirm that, at the length scale of the µCR (ca. 100 µm), the effect of the increased surface-to-volume ratio is still not relevant [13]. Fig. 3 demonstrates the ability of µCR to correctly measure the viscosity over a wide range of shear rates (from 0.1 to 1000s^{-1}, viscosity from 10 to 10^5 Pa s) and temperatures (from 25 °C to 200 °C). It is worth noting that the each set of viscosity data has been measured using only 12 mg of material. In all cases, the measurement of the entire flow curves is achieved in ca. 10 min.

8. Extrudate swell

The extrudate swell can be observed by using the same videocamera that measures the flow rate. It should be remarked that, due to the micrometric dimension of the strand, gravitational effects are negligible. The same is true for the surface tension effects, as $Ca \gg 1$. Furthermore, as the strand coming out of the orifice is collected in a closed chamber, its temperature can be maintained at constant value so avoiding sample cooling. For the above reasons the extrudate swell can be calculated as $B = \frac{D_s}{D}$, where D_s is the diameter of the extrudate. The swell measurements can be considered independent of the geometry because the µCR design is characterized by $R_r/R < 10$ and $L/R > 10$, where R_r is the radius of the cylindrical reservoir [22]. The die swell can be related to the first normal stress difference, N_1, and it is often used as a normal stress index [23]-. However, the relation found by Tanner [23] between die swell and N_1 is model-dependent, on the basis of not rigorous assumptions. By estimating N_1 with the empirical relationship $N_1^2 = 8\tau_w^2((B-0.13)^6 -1)$ we obtain the first normal stress coefficient, ψ_1, reported in Fig. 4 for the PS at 180 °C. As expected, ψ_1 approaches a constant value at low shear rates and decreases dramatically with increasing shear rate. For comparison, we also report ψ_1 evaluated from dynamic data by using Laun's rule [35]. A good agreement is observed between the two estimates. The measured extrudate swell in the shear range from 10 to 1000 s^{-1} is comparable (within an error of ca. 20%) to literature values for PS [25]. At low shear rates the polymer wets the metal surface and the measurement error for the die swell increases. The use of coatings to avoid the wetting on the metal surface will help to extend the die swell
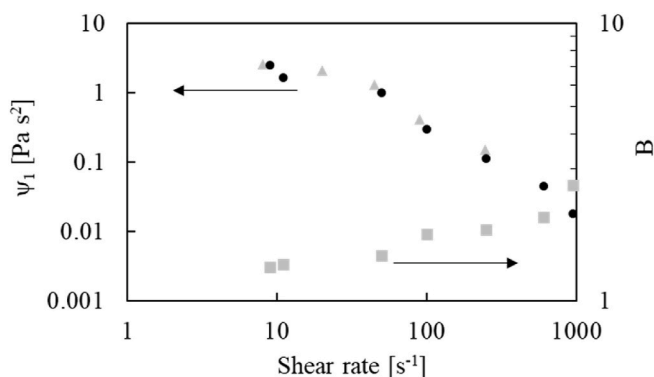

Fig. 4. First normal stress difference coefficient, ψ1 (black circles), as function of shear rate for PS at 200 °C calculated from the extrudate swell, B (grey squares). First normal stress difference coefficient (grey triangles) as function of shear rate for PS at 200 °C calculated with Laun's rule [35].

measurements at low shear rates.

9. Contact angle and surface tension

The µCR also offers the possibility to measure surface properties of the fluids, still using milligram size polymers, in a controlled temperature and pressure chamber. As a proof-of-concept we measured the contact angle of POE on a milled metal surface. The contact angle can be measured by depositing a small drop of material on the solid surface (sessile drop). Alternatively, a small amount of liquid can be pushed through the capillary to form a small drop at the capillary exit (pendant drop). In both cases, care must be taken to wait for the reaching of steady-state conditions. In the case of polymer sessile drops on solid surfaces, the equilibrium contact angle is approached within a time interval that varies from minutes to hours, depending on the temperature and the system examined [26]. Equilibrium is reached after the characteristic time for the interfacial-tension-driven motions $t_c \sim \frac{\eta}{\gamma} R_d \sim 1000s$, where η is the zero-shear viscosity of the POE at 180 °C, γ is the surface tension and R_d is the sessile drop radius [27]. It should be stressed that the µCR design avoids polymer degradation by nitrogen purge in the measurement chamber. Needless to say, the contact angle can be measured on different substrates by changing the surface material.

Snapshots of the droplet were taken under equilibrium conditions (Fig. 5a) and the contact angle was calculated by the telescope-goniometer method [28]. The latter allows for a direct measurement of the line tangent to the drop profile in the triple contact point. The contact angle at different temperatures under nitrogen flux on the milled metal (stainless steel 1.4305) surface are reported in Fig. 5b. The contact angle is deduced by the tangent at the triple point because, in our conditions, the ratio between the Laplace pressure and the hydrostatic pressure is much greater than unity (the capillary length, $\sqrt{\frac{\gamma}{\rho g}} \gg R$, where ρ is the fluid density [29]) and gravity effects can be considered as negligible. Using a similar procedure, it is possible to measure the surface tension by the pendant drop method [30]. The measured data are shown in Fig. 5c. A similar qualitative dependency of the contact angle and surface tension with the temperature was reported by Zitzenbacher et al. [34] for polypropylene and polymethylmethacrylate on polished steel at high temperature.

10. Melt fracture

The µCR can also be used to investigate processability limits. The onset of melt instabilities was observed with POE melts at 150 °C. No instabilities were detected for PDMS and PS in the temperature and shear rates ranges used in the measurements. It is well known that
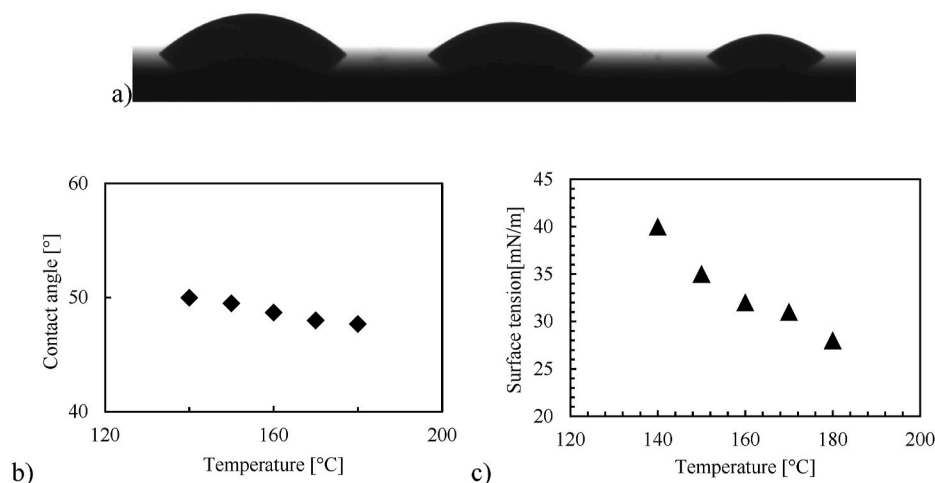
Fig. 5. a) snapshot of three droplets at the microcapillaries exit and b) contact angle measurements at different temperatures for POE.

polymer melts exiting from pipes show a transition from stable to unstable flow at high stress, known as melt fracture [31]. A definitive theory describing this phenomenon is not yet available, as well as the corresponding transition from regular to irregular patterns on the extrudate surface. Usually, this transition is attributed to the attaining of a critical limiting shear stress at the wall. Using the μCR with a microcapillary of 70 μm it was possible to investigate the onset of melt fracture and the patterns produced on the surface. The investigation of the patterns is here simplified since the microstrands can be frozen in a very short time (the characteristic heat diffusion time for the 70 μm strand is $\tau_d = \frac{(R)^2}{a} \sim 1s$, where a is the thermal diffusivity of the fluid). Consequently, the melt fracture can be characterized either inline by an optical camera (Fig. 5a) or off-line by post-extrusion SEM. The latter can be used to collect more details on the formed patterns at different levels of shear stress (Fig. 6b and c).

The measured onset of melt fracture for the investigated POE is $\sim 3 \times 10^5 Pa$. Such a value is in line with the expected value for linear low-density polyethylene [32]. Needless to say, the appearance of melt instability represents the limit for the viscosity measurement [17]. The shear rate dependence of shear stresses for POE is shown in Fig. 6d, and the vertical lines separate smooth, periodic and melt fracture regimes.

11. Error analysis

In this section, the different factors that determine the μCR measurement uncertainty are analysed. The uncertainty can be divided into a systematic part related to the instrument settings, such as temperature and pressure control, and a random part, linked to the inevitable experimental scattering.

Within the instrument settings, a relevant factor is the accuracy of the capillary geometry. The capillary diameter, in particular, is a crucial parameter in view of the fourth power effect on the viscosity. The diameter, the eccentricity and the roughness of the microcapillary were measured by SEM analysis, as shown in Fig. 7a for the case of 70 μm capillary. The images return a diameter of 70 μm with essentially no eccentricity and roughness of ca. 1 μm. To measure the actual length of the capillary, a mould was obtained by carefully removing the solidified polymer inside the cavity (Fig. 7b). The nominal and calculated geometrical parameters for all the capillaries used in this work are shown in Table 2.

Regarding the error related to the optical technique to determine the liquid flow rate, relevant camera parameters are the frame rate, field of view, and resolution. In our tests we used a commercial, quite unexpensive camera with 130fps, 2.0x lens, 2MPixel, which supplies a sufficient data sampling up to a shear rate of $1000s^{-1}$ for the capillary of 70

μm, for a minimum volume measurement in the order of 1 μL. The fluid volume is measured by integrating the area of the strand coming out of the microcapillary. The accuracy of the numerical integration was checked for the PDMS fluid by comparing the measured volume with that obtained by weighting the extruded mass making use of the PDMS density [33,36]. The relative error between the two measurements of the volume was ca. 1%. The assumption of axial symmetry off the measured object, used in the numerical integration, is crucial and it becomes critical for very high shear rates (larger than $1000s^{-1}$), where the strand distortion becomes relevant, and the strand exits from the field of view. In those cases, the flow rate can be calculated by tracking particles or defects in the strand by assuming a plug flow condition out of the orifice.

Finally, we validated the accuracy of the flow rate measurements through a comparison with simulation results. A Newtonian fluid, with a constant kinematic viscosity of 1000000 cSt is considered. The finite element method is employed to solve the mass and momentum balance equations under inertialess assumptions. The three capillaries with diameter D = 400 μm and land length L = 2, 3, 4 mm are simulated with applied pressure drops ranging from 0.8 to 5.3 bar. Fig. 7c shows the relative error between the experimental and simulated flow rates. For the investigated conditions, the relative error is always below 3%, thus validating the accuracy of the experimental technique.

The evaluation of the random error is obtained from repeated experiments (10 replicated measurements) and the resulting standard deviation is ca. 5%.

12. Conclusions

We presented a novel microcapillary rheometer capable of performing several experiments in parallel handling just few milligrams polymer, thus allowing for HT-Rheo-E characterization. The stress-imposed device is able to perform experiments rapidly and on a broad range of shear rates (presently, from 0.1 to 1000 s^{-1}). We prove the reliability of viscosity measurements by comparison with data from a rotational rheometer. Additionally, it was shown that μCR can also serve to the characterization of other fluid properties, e.g., die swell, contact angle, and possible melt fracture.

Therefore, it represents a cost-effective, easy to manage and reliable instrument for the rheological characterization of milligram size polymers.
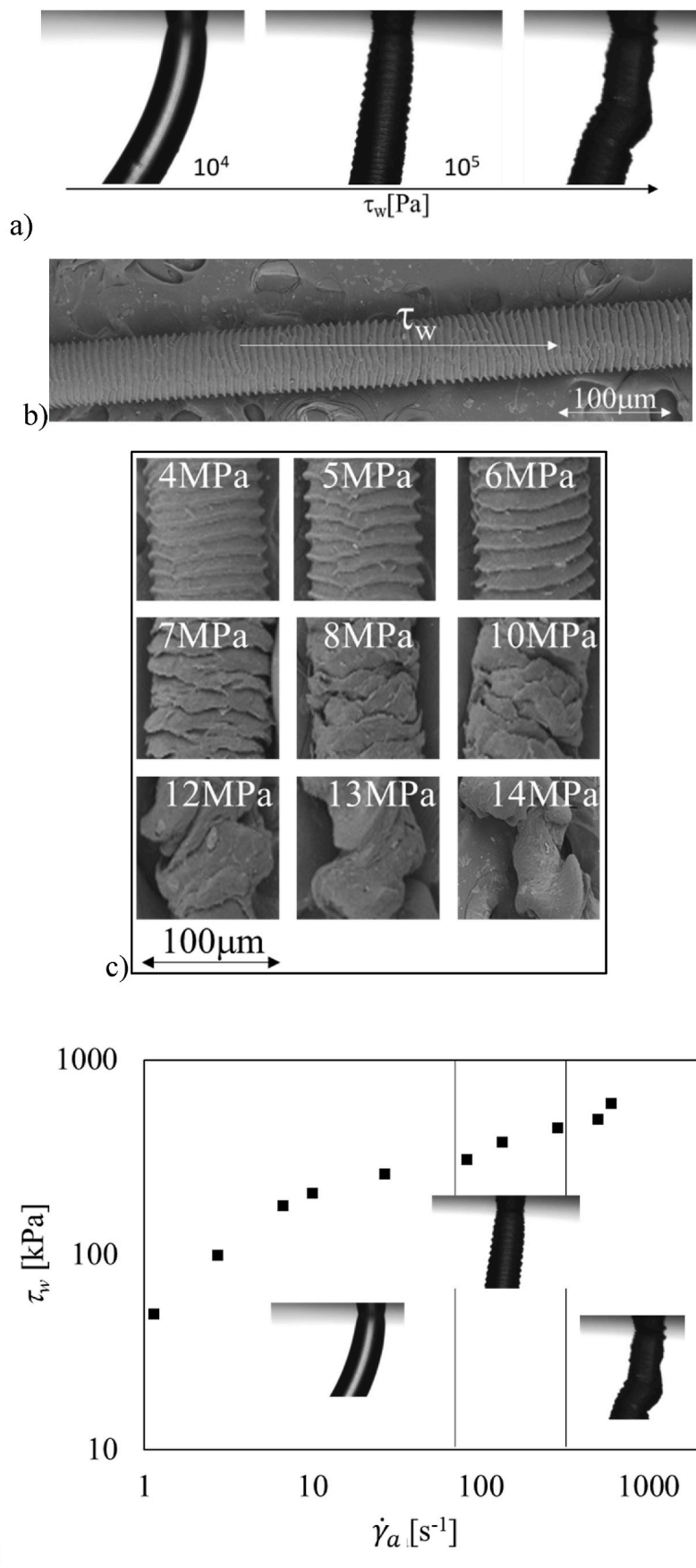
Author statement

Fig. 6. a) inline measurement of melt instability, b) SEM image of microstrand at the onset of melt fracture, c) evolution of melt fracture at several pressure drop, d) shear stresses as function of apparent shear rate for POE, the insets are real images of the polymer strand.
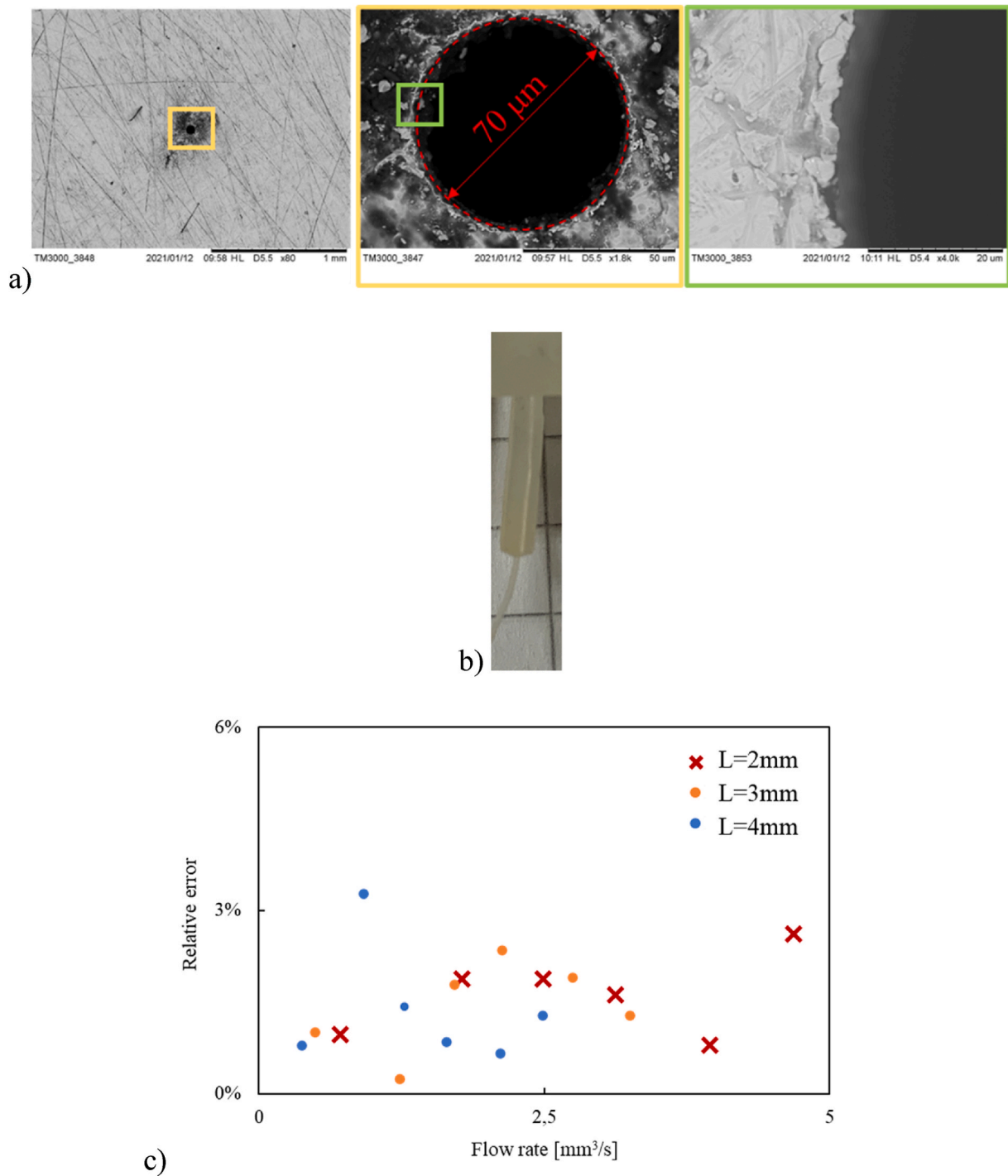
a)

b)

c)

Fig. 7. a) SEM of the exit section of microcapillary with 3 magnifications from left to right: 80x – 1800x – 4000x, b) mould of the capillary obtained with the POE used for the test, c) relative error between the simulated and measured flow rate for three different land length.

Table 2
Geometry of the capillaries.

Nominal diameter x nominal length	Diameter [mm]	Length [mm]
0.07x0.450	0.07 ± 0.002	0.455 ± 0.005
0.400x2	0.405 ± 0.005	2 ± 0.05
0.400x3	0.404 ± 0.005	3 ± 0.07
0.400x4	0.407 ± 0.005	4 ± 0.06

Declaration of competing interest

The authors declare that they have no known competing financial interests or personal relationships that could have appeared to influence the work reported in this paper.

References

[1] J.J. Hanak, The "multiple-sample concept" in materials research: synthesis, compositional analysis and testing of entire multicomponent systems, J. Mater. Sci. 5 (1970) 964–971.

[2] Jatin N. Kumar, Qianxiao Li, Jun Ye, Challenges and opportunities of polymer design with machine learning and high throughput experimentation, MRS Commun. 4 (2019) 537–544.

[3] Jeffrey D. Martin, et al., Interfacial rheology through microfluidics 10 (2011) 426–432.

[4] Pietro Cicuta, Athene M. Donald, Microrheology: a review of the method and applications, Soft Matter 3 (2007) 1449–1455.

[5] C.J. Pipe, G.H. McKinley, Microfluidic rheometry, Mech. Res. Commun. 36 (2009) 110–120.

[6] Daniele Tammaro, Salvatore Iannace, Ernesto Di Maio, Insight into bubble nucleation at high-pressure drop rate, J. Cell. Plast. 53 (5) (2017) 551–560.

[7] D. Moon, K.B. Migler, Measurement of dynamic capillary pressure and viscosity via the multi-sample micro-slit rheometer, Chem. Eng. Sci. 64 (2009) 4537–4542.

[8] Doyoung Moon, Anthony J. Bur, Kalman B. Migler, Multi-sample micro-slit rheometry, J. Rheol. 52 (2008) 1131–1142.

[9] S. Costanzo, R. Pasquino, J. Läuger, N. Grizzuti, Milligram size rheology of molten polymers, Fluids 4 (2019) 28.

[10] J.J. Benbow, P. Lamb, Rheological measurements on polymer melts using very small samples, J. Sci. Instrum. 414 (1964) 203–205.

[11] Y.M. Ybarra, R.E. Eckert, Viscous heat generation in slit flow, AIChE J. 26 (1980) 751–762.

[12] H. Shidara, M.M. Denn, Polymer melt flow in very thin slits, J. Non-Newtonian Fluid Mech. 48 (1993) 101–110.

[13] Christian Clasen, Gareth H. McKinley, Gap-dependent microrheometry of complex liquids, J. Non-Newtonian Fluid Mech. 124 (2004) 1–10.

[14] Doyoung Moon, Kalman B. Migler, Measurement of dynamic capillary pressure and viscosity via the multi-sample micro-slit rheometer, Chem. Eng. Sci. 64 (2009) 4537–4542.

[15] E.R.G. Eckert, M. Faghri, Viscous heating of high Prandtl number fluids with temperature-dependent viscosity, Int. J. Heat Mass Tran. 29 (1986) 1177–1183.

[16] Evan Mitsoulis, Savvas G. Hatzikiriakos, Bagley correction: the effect of contraction angle and its prediction, Rheol. Acta 24 (2003) 309–320.

[17] Christopher W. Macosko, Rheology Principles., Measurements and Applications, VCH Publishes, 1994.

[18] C.D. Han, Entrahce region flow of polymer melts, AIChE 17 (1971) 1480–1496.

[19] A.B. Metzner, J.L. White, Flow behavior of viscoelastic fluids in the inlet region of a channel, AIChE J. 11 (1965) 989–995.

[20] Z. Wang, B. Mandracchia, V. Ferraro, D. Tammaro, E. Di Maio, P.L. Maffettone, P. Ferraro, Interferometric measurement of film thickness during bubble blowing, in: Optical Methods for Inspection, Characterization, and Imaging of Biomaterials III, vol. 10333, International Society for Optics and Photonics, 2017, June, p. 103331O.

[21] Pierre Guillot, Annie Colin, Determination of the flow curve of complex fluids using the Rabinowitsch–Mooney equation in sensorless microrheometer, Microfluid. Nanofluidics 17 (2014) 605–611.

[22] C.D. Han, Rheology in Polymer Processing, Academic Press, New York, 1976, 5th Chapter.

[23] Roger I. Tanner, A theory of die-swell revisited, J. Non-Newtonian Fluid Mech. 129 (2005) 85–87.

[24] D. Tammaro, V.C. Suja, A. Kannan, L.D. Gala, E. Di Maio, G.G. Fuller, P. L. Maffettone, Flowering in bursting bubbles with viscoelastic interfaces, Proc. Natl. Acad. Sci. Unit. States Am. 118 (30) (2021).

[25] L. Lombardi, D. Tammaro, Effect of polymer swell in extrusion foaming of low-density polyethylene, Phys. Fluids 22 (2021) 33–44.

[26] D. Tammaro, E. Di Maio, Early bubble coalescence in thermoplastic foaming, Mater. Lett. 228 (2018) 459–462.

[27] D. Tammaro, C. Walker, L. Lombardi, U. Trommsdorff, Effect of extrudate swell on extrusion foam of polyethylene terephthalate, J. Cell. Plast. (2020), 0021955X20973599.

[28] Yuehua Yuan, T. Randall Lee, Contact Angle and Wetting Properties, Surface Science Techniques, vol. 5, Springer, Berlin, Heidelberg, 2013, pp. 3–34.

[29] P.G. De Gennes, Françoise Brochard-Wyart, D. Quéré, Capillarity and Wetting Phenomena: Drops, Bubbles, Pearls, Waves, Springer Science & Business Media, 2013.

[30] M.G.P. Carbone, D. Tammaro, A.C. Manikas, G. Paterakis, E. Di Maio, C. Galiotis, Wettability of graphene by molten polymers, Polymer 180 (2019) 121708.

[31] Rudy Koopmans, Jaap Den Doelder, Jaap Molenaar, Polymer Melt Fracture, CRC Press, 2010.

[32] J.P. Tordella, Capillary flow of molten polyethylene—a photographic study of melt fracture, Trans. Soc. Rheol. 1 (1957) 203–212.

[33] Polymer Data Handbook, Mark J., Oxford Univ. Press, New York, 1999.

[34] Gernot Zitzenbacher, Hannes Dirnberger, Manuel Längauer, Clemens Holzer, Calculation of the contact angle of polymer melts on tool surfaces from viscosity parameters, Polymer 10 (2017) 38–45.

[35] H.M. Laun, Prediction of elastic strains of polymer melts in shear and elongation, J. Rheol. 30 (1986) 459–501.

[36] D. Tammaro, L. Lombardi, G. Scherillo, E. Di Maio, N. Ahuja, G. Mensitieri, Modelling sorption thermodynamics and mass transport of n-hexane in a propylene-ethylene elastomer, Polymers 13 (7) (2021) 1157.